doi:10.6041/j.issn.1000-1298.2016.01.006

Motion Analysis of Tractor Robot Driver's Gear Shift Mechanical Arm

Lu Wei[1,2] Chen Hao[1] Wang Ling[1] Zhao Xianlin[1] Zhang Yongnian[1]

(1. *College of Engineering, Nanjing Agricultural University, Nanjing* 210031, *China*
2. *Key Laboratory of Remote Control and Measurement Technology in Jiangsu Province, Nanjing* 210096, *China*)

Abstract: Respect to the character that the gearbox shifting resistance in the four-wheel minitype agricultural tractor is time-varying and nonlinear and the special requirement that the gear shift lever has to be released after shifting, this paper designed a novel gear shift mechanical arm for tractor robot driver. This manipulator is joint type. According to the manipulator's operating characteristic, this paper applied D-H method to establish the coordinate transformation matrix. Based on the kinematics analysis on the manipulator, Lagrange equation was used to simplify kinetic model of the manipulator. SolidWorks and ADAMS were applied to establish the virtual prototype model of the manipulator and to do kinematic and dynamic simulation respectively. In order to guarantee the smoothness of shift, the distance between the terminal of the manipulator's actuator and the gear shift lever of the tractor was set to less than 50 mm. The absolute value of terminal actuator's minimum jitter speed during shift was optimized as the objective function. The target function is optimal when the length of shift manipulator is 220.0 mm and the height of the terminal is 393.25 mm. After optimization, the jitter speed fluctuation is 28.18% less than before. The rate of change of average displacement and average acceleration are 49.55% and 52.05%. At the same time, the peak value of the displacement, velocity and acceleration are 60.22%, 66.24% and 81.66% respectively. Through the simulation, the optimization of the parameters of the manipulator, the rationality and the scientificity of the model are verified. Finally, through the experiment on gear shift mechanical arm on JINMA 300E tractor, the result shows that the gear mechanical arm can realize the goal to shift different gears smoothly. In addition, the design of the gear mechanical arm can complete some complicated actions of tractor's driver. Thus, the gear shift mechanical arm has excellent engineering and application value.

Key words: tractor; robot driver; gear shift; motion simulation; parameter optimization

0 Introduction

In China, the development of automation and intelligence of tractor still lags behind relatively. Till now, a lot of valuable studies have been done by researchers on how to introduce intelligent control based on multiple sensors to the traditional driving of tractor. For example, some researchers from Hokkaido University, University of Illinois, Ehime University, South China Agricultural University, China Agricultural University, Nanjing Agricultural University and other universities have researched on the unmanned agricultural tractor[1-3], related to the reformation of the implementation of the tractor and driving control. In addition, certain partial products in Deere, CNH, AGCO, Kubota and FENTE also have unmanned function[4-5]. But the tractor needs to be done the second transformation to become intelligent tractor, whose cost is high. At the same time, once the tractor is damaged, the smart devices installed on it are difficult to transplant to other tractors. Comparatively speaking, the development of robot driver technology provides an opportunity to solve the problem of agricultural intelligence. At present, using robot driver to replace human driver to complete the car driving operation has become a development tendency in

Received date: 2015-07-20 Accepted date: 2015-10-08

Supported by National Natural Science Foundation of China (Grant No. 51405239), Natural Science Foundation of Jiangsu Province (Grant No. BK20130696), Fundamental Research Funds for the Central Universities (Grant No. KYZ201427), and Open fund of Jiangsu Province Key Laboratory for Remote Measuring and Control (Grant No. YCCK201501)

Corresponding author: Lu Wei, Associate professor. E-mail: njaurobot@njau.edu.cn. Tel: +86-25-58606595.

vehicle testing industry. Robot driver which composed of gear shift mechanical arm, clutch mechanical leg, brake mechanical leg and accelerator mechanical leg has developed into an integrated system. Each actuator can be installed individually and completed the corresponding test experiments. Apparently, robot driver has become an essential intelligent device in modern automobile experiments[6]. Nowadays, pure electric robot driver of some companies such as HORIBO, Nissan Motor, AUTOMAX, SCHENCK, MIRA have been developed which can substitute for the human driver in road test. Domestic and international robot driver is basically occupied by foreign companies' products while such research is still relatively little in China[7-10].

Due to the special mechanical structure of the tractor, there are few reports about applying robot technology to the four-wheel tractor. It has important practical significance and scientific value to do non-destructive and intelligent upgrade to the traditional agricultural tractor by researching the wide universality and high-performance tractor robot driver. Tractor structure and vehicle are significantly different because of its low price and great pulling force. One of the technical difficulties to realize automatic shifting is that it is hard to control the manual gearbox of the tractor robot driver. At the same time, the joystick must be released after shifting. This paper focuses on the technical difficulties of the automatic shifting of the gearbox in the four-wheel agricultural tractor's intelligent upgrading. Based on that, gear shift mechanical arm are designed and theoretical and experimental studies are carried on.

1 Design of tractor driver robot's gear shift mechanical arm

1.1 Demand parameter analysis

At present, most medium and large tractors widely adopt synchronizer to shift while most small tractors apply mechanical manual gearbox to shift[11-12]. The shifting process is that shifting fork toggles the sliding gear to make the gear mesh or separate with relative gear. The ball head supports the joystick to make sure that the lower end of the transmission can complete front-to-back motion and side-to-side motion. When the joystick is doing front-to-back motion, the shifting fork will be driven to move the sliding gear. Until the sliding gear is in place, it should be locked. When the joystick is doing side-to-side motion, the lower end of that will be moved in the slot, the resistance of selection is small and smooth.

Compared with the automobile gearbox, the shifting resistance of tractor's gearbox is larger because of the larger sliding gear in the small tractor gearbox, the meshing force and non-simultaneous impact. When shifting, shifting fork toggles sliding gear to make tooth of face mesh with tooth of shaft. Then active force of engine will be transferred to the corresponding shaft. After the sliding gear engages with the shaft gear, the joystick has to be released to ensure the stability of shifting and to prolong the operating life. The mechanism of shifting is shown in Fig. 1.

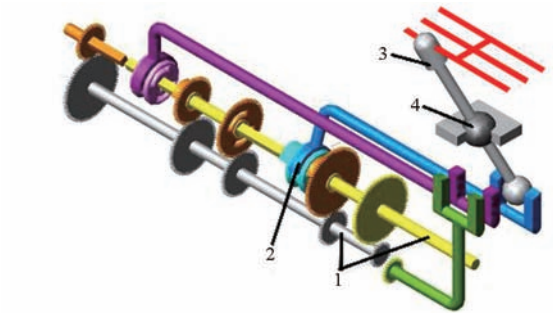

Fig. 1 Shifting mechanism

1. Shaft 2. Fork-level 3. Joystick 4. Ball support

The *XY* electric linear sliding table driven by step motor was fixed on the top of the working space of the joystick. The working plane of sliding table linked with joystick of tractor through force sensor. Based on such structure, the actual shifting distance and shifting resistance can be measured. Through the measurement, the range of the joystick's end is about 200 mm in the direction of *X* and 85 mm in the *Y* direction respectively. The tractor's main wheel would be launched and suspended in midair. The shifting resistance of shifting from neutral gear to other gears was shown in Fig. 2.

At the moment of the change of the gear shifting, the

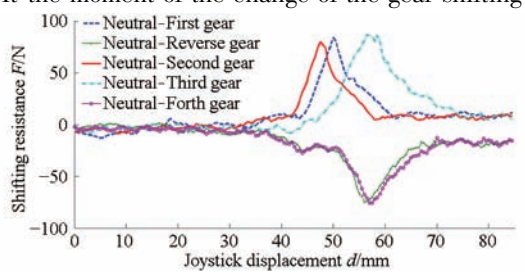

Fig. 2 Curves of shifting resistance

shifting resistance reached a peak value of about 80 N. That shifting resistance had time varying, nonlinear and other significant characteristics.

1.2 Structure design

According to the above-mentioned analysis and the requirements of shifting parameters of gear shift mechanical arm, the mechanical structure of the tractor driver robot's gear shift mechanical arm is illustrated in Fig. 3. The gear shift mechanical arm is composed of X direction actuator and Y direction actuator. The X direction actuator chose CY - 42YT200 type linear light rod guide slide table and 42H4812 two-phase hybrid stepping motor whose torque was 0.5 N·m and accuracy was 0.1 mm. Y direction actuator applied electric putter with gain encoder whose stroke was 300 mm and thrust was 250 N. X direction actuator and the Y direction actuator were connected through the connecting piece. X direction slide table can drive Y directions actuator to reach any selecting gear position of joystick and fix with it precisely. The electric putter of Y direction can control shift lever to reach any shifting position, thus realizing the motion decoupling of the two directions of the mechanical arm. Force sensor which was installed in front of the terminal of the mechanical arm can measure the push-pull effort during shifting process. Clamping device was sleeve which was made of plastic material. The sleeve whose diameter is slightly larger than shift lever's held the terminal of the shift lever. So shift lever can do mini free movement after it went into place to simulate the release action approximately after completing shifting. In such as, there was no friction in tractor's shifter.

Fig. 3 Three-dimensional model of tractor driver robot's gear shift mechanical arm

1. Step motor 2. Lead screw 3. Slider 4. Hinge 5. Electric pusher 6. Force sensor 7. Cylinder(Joystick holder)

2 Kinematics and dynamics analysis of mechanical arm

2.1 Positive solution of mechanical arm kinematics

In this paper, the mechanical arm is equivalent to a joint type manipulator and a coordinate system is fixed at the joint. The relative position and attitude of the coordinate system are described by D - H method[13]. In order to reduce the amount of computation, we did an equivalent treatment and gave four coordinate systems. The coordinate system of mechanical arms is shown as Fig. 4 below. Among them, $O_0X_0Y_0Z_0$ is a base coordinate—a coordiante that is the shifting position in linear guide rail of slide table. l_2 is the distance in Y direction of slide table. $O_2X_2Y_2Z_2$ is the coordinate system when $O_1X_1Y_1Z_1$ rotating θ_2 angle. d_3 is the moving distance of the manipulator in X direction. $O_3X_3Y_3Z_3$ is a coordinate system which is used for describing the position of manipulator in the end actuator of the mechanical arm.

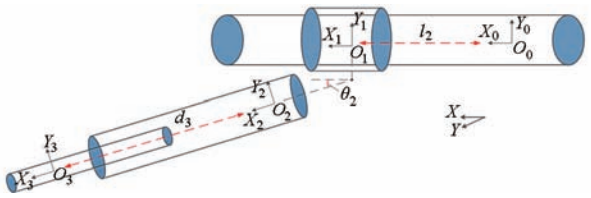

Fig. 4 Coordinate system of mechanical arm

According to the D - H method, for the extreme rod of kinematic chain, the parameters are set to 0. According to Fig. 4, the parameters of connecting rod of the mechanical arm are shown in Tab. 1.

Tab. 1 Link parameters of mechanical arm

i	α_{i-1}	a_{i-1}	d_i	θ_i
1	0	0	0	0
2	0	0	l_2	θ_2
3	0	d_3	0	0

Put the general expressions of the parameters into the transformation matrix ${}_i^{i-1}\boldsymbol{T}$.

$$ {}_i^{i-1}\boldsymbol{T} = \begin{pmatrix} c\theta_i & -s\theta_i & 0 & a_{i-1} \\ s\theta_i c\alpha_{i-1} & c\theta_i c\alpha_{i-1} & -s\alpha_{i-1} & -s\alpha_{i-1} d_i \\ s\theta_i s\alpha_{i-1} & c\theta_i s\alpha_{i-1} & c\alpha_{i-1} & c\alpha_{i-1} d_i \\ 0 & 0 & 0 & 1 \end{pmatrix} \tag{1} $$

and

$$\begin{cases} {}^{0}_{1}\boldsymbol{T} = \begin{pmatrix} 1 & 0 & 0 & 0 \\ 0 & 1 & 0 & 0 \\ 0 & 0 & 1 & 0 \\ 0 & 0 & 0 & 1 \end{pmatrix} \\ {}^{1}_{2}\boldsymbol{T} = \begin{pmatrix} c\theta_2 & -s\theta_2 & 0 & 0 \\ s\theta_2 & c\theta_2 & 0 & 0 \\ 0 & 0 & 1 & l_2 \\ 0 & 0 & 0 & 1 \end{pmatrix} \\ {}^{2}_{3}\boldsymbol{T} = \begin{pmatrix} 1 & 0 & 0 & d_3 \\ 0 & 1 & 0 & 0 \\ 0 & 0 & 1 & 0 \\ 0 & 0 & 0 & 1 \end{pmatrix} \end{cases} \tag{2}$$

$${}^{0}_{3}\boldsymbol{T} = {}^{0}_{1}\boldsymbol{T}^{1}_{2}\boldsymbol{T}^{2}_{3}\boldsymbol{T} = \begin{pmatrix} c\theta_2 & -s\theta_2 & 0 & d_3 c\theta_2 \\ s\theta_2 & c\theta_2 & 0 & d_3 s\theta_2 \\ 0 & 0 & 1 & l_2 \\ 0 & 0 & 0 & 1 \end{pmatrix} \tag{3}$$

In such expressions, $s\theta_2$ means $\sin\theta_2$ and $c\theta_2$ means $\cos\theta_2$.

The kinematic equation represents the space position and direction vector of the terminal actuator of the mechanical arm and the transformation relationship between the pose and the parameters of those various components.

2.2 Inverse kinematics of mechanical arm

The inverse kinematics of the motion required the relative transformation between the Cartesian space and the base coordinate system of the terminal actuator. Through using established amount, the joint angle θ_2 can be determined. The transformation matrix ${}^{0}_{3}\boldsymbol{T}$, which was used to determine the target point, was described as

$${}^{0}_{3}\boldsymbol{T} = \begin{pmatrix} c\theta_2 & -s\theta_2 & 0 & x \\ s\theta_2 & c\theta_2 & 0 & y \\ 0 & 0 & 1 & l_2 \\ 0 & 0 & 0 & 1 \end{pmatrix} \tag{4}$$

Such formulas can be detrivated

$$\tan\theta_2 = \frac{y}{x} \tag{5}$$

$$\theta_2 = \arctan\frac{y}{x} \tag{6}$$

By analyzing the kinematics of the mechanical arm, the projection of work space of shifting lever and mechanical arm can be attained as Fig. 5. The shift lever's motion projection of the selecting direction and the shifting direction are $-100 \sim 100$ mm and $0 \sim 85$ mm respectively. Apparently, the projected area is 17 000 mm^2. The mechanical arm's horizontal projection of X direction and Y direction are $-120 \sim 120$ mm and $0 \sim 100$ mm respectively. The projected area is 24 000 mm^2. From Fig. 5, it can be known that the working space of the mechanical arm covered the working space of the joystick completely. It can meet the requirements of shifting. The simulation verified the scientificity and rationality of the structural design and kinematics of the mechanical arm.

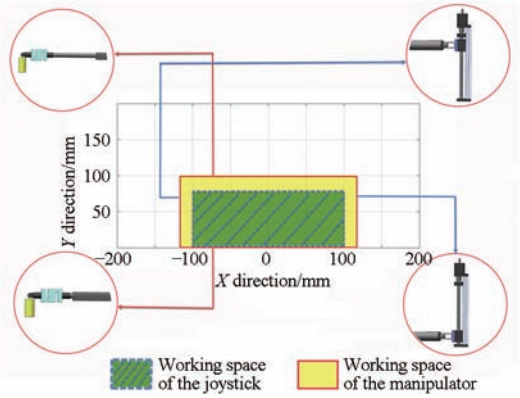

Fig. 5 Working space of gear shift mechanical arm

2.3 Mechanical analysis of mechanical arm

Lagrange dynamic formula gives a method to derive dynamic equation from scalar function[14]. This scalar function is the Lagrange function. In this paper, the Lagrange function of the mechanical arm is expressed as

$$L(\boldsymbol{\Theta}, \dot{\boldsymbol{\Theta}}) = k(\boldsymbol{\Theta}, \dot{\boldsymbol{\Theta}}) - u(\boldsymbol{\Theta}) \tag{7}$$

Then, the motion equation of the mechanical arm is expressed as[15]

$$\frac{\mathrm{d}}{\mathrm{d}t}\frac{\partial L}{\partial \dot{\boldsymbol{\Theta}}} - \frac{\partial L}{\partial \boldsymbol{\Theta}} = \boldsymbol{\tau} \tag{8}$$

From Eqs. (7) and (8), Eq. (9) can be attained as

$$\frac{\mathrm{d}}{\mathrm{d}t}\frac{\partial k}{\partial \dot{\boldsymbol{\Theta}}} - \frac{\partial k}{\partial \boldsymbol{\Theta}} + \frac{\partial u}{\partial \boldsymbol{\Theta}} = \boldsymbol{\tau} \tag{9}$$

Where $k(\boldsymbol{\Theta}, \dot{\boldsymbol{\Theta}})$ is the kinect energy of mechanical arm; $u(\boldsymbol{\Theta})$ is the potential energy; $\boldsymbol{\tau}$ is a $n \times 1$ dimensional driving force vector ; $\boldsymbol{\Theta}$ is the joint position.

By applying the method of lumped mass, the actuator in Y direction of the mechanical arm was simplified as Fig. 6. The dynamics degrees of freedom of mechanical arm is 2, whose quality of back end is m_1. The quality of extending end, force sensor and clamping device is m_2. The distance between

barycenter and the axis of the joint is l_1. The distance between barycenter of the extending end, force sensor and clamping device and the axis of the joint is variable d_2.

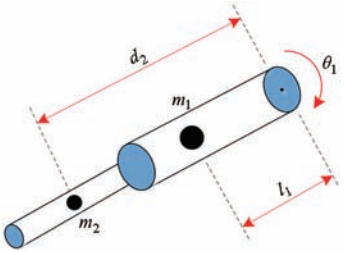

Fig. 6 Motion diagram of mechanical arm in Y direction

The inertia tensor of the back end and the extended end of the mechanical arm can be expressed as

$$\begin{cases} {}^{C_1}\boldsymbol{I}_1 = \begin{pmatrix} I_{xx1} & 0 & 0 \\ 0 & I_{yy1} & 0 \\ 0 & 0 & I_{zz1} \end{pmatrix} \\ {}^{C_2}\boldsymbol{I}_2 = \begin{pmatrix} I_{xx2} & 0 & 0 \\ 0 & I_{yy2} & 0 \\ 0 & 0 & I_{zz2} \end{pmatrix} \end{cases} \tag{10}$$

In order to simplify the calculation, the mechanical arm was equivalent to the mass of a homogeneous entity approximately. The elements of the Eq. (10) matrix can be expressed as

$$\begin{cases} I_{xx} = \iiint_V (y^2 + z^2)\rho \mathrm{d}v \\ I_{yy} = \iiint_V (x^2 + z^2)\rho \mathrm{d}v \\ I_{zz} = \iiint_V (x^2 + y^2)\rho \mathrm{d}v \end{cases} \tag{11}$$

The kinetic energy at the back end of the mechanical arm is shown as

$$k_1 = \frac{1}{2} m_1 l_1^2 \dot{\theta}_1^2 + \frac{1}{2} I_{zz1} \dot{\theta}_1^2 \tag{12}$$

The kinetic energy of the extending end, force sensor and clamping device is shown as

$$k_2 = \frac{1}{2} m_2 (d_2^2 \dot{\theta}_1^2 + \dot{d}_2^2) + \frac{1}{2} I_{zz2} \dot{\theta}_1^2 \tag{13}$$

The total kinetic energy can be attained from Eqs. (12) and (13)

$$k(\boldsymbol{\Theta}, \dot{\boldsymbol{\Theta}}) = \frac{1}{2} (m_1 l_1^2 + I_{zz1} + I_{zz2} + m_2 d_2^2) \dot{\theta}_1^2 + \frac{1}{2} m_2 \dot{d}_2^2 \tag{14}$$

The potential energy of the mechanical arm is shown as

$$u_1 = m_1 l_1 g \sin\theta_1 + m_1 l_1 g \tag{15}$$

The potential energy of the extending end, force sensor and clamping device is shown as

$$u_2 = m_2 d_2 g \sin\theta_1 + m_2 g d_{2\max} \tag{16}$$

In Eq. (16), $d_{2\max}$ is the maximum range of motion of the end actuator. The total potential energy can be attained from Eqs. (15) and (16)

$$u(\boldsymbol{\Theta}) = (m_1 l_1 + m_2 d_2) g \sin\theta_1 + m_1 l_1 g + m_2 g d_{2\max} \tag{17}$$

By putting partial derivatives into the Eq. (9), the final dynamic equations of the mechanical arm can be expressed as

$$\boldsymbol{\tau}_1 = (m_1 l_1^2 + I_{zz1} + I_{zz2} + m_2 d_2^2) \ddot{\theta}_1 + 2 m_2 d_2 \dot{\theta}_1 \dot{d}_2 + (m_1 l_1 + m_2 d_2) g \cos\theta_1 \tag{18}$$

$$\boldsymbol{\tau}_2 = m_2 \ddot{d}_2 - m_2 d_2 \dot{\theta}_1^2 + m_2 g \sin\theta_1 \tag{19}$$

A virtual prototype model of the gear shift mechanical arm was built by SolidWorks. This was imported into ADAMS as Fig. 7. Characteristics parameters of different parts in the mechanical arm model were set according to the physical prototype material. Based upon the joint movement, the relative constraint of motion was applied. In order to validate the correctness of the dynamics model, the simulation process should consider not only the meshing force of gearbox and resistance of the self-locking device. According to the experiments of ractor shifting, the shifting of the manual transmission gear can be completed only when it was equipped with operation of clutch. Especially when shifting from higher gear to lower gear, in order to avoid the damage of the gear collision, the clutch must be separated twice. At the same time, the resistance at the moment of entry would be decreased obviously[16]. During the process of simulation in ADAMS, the sensor was created. The mechanical arm was controlled to stop when the sliding gear of gearbox enter in right place.

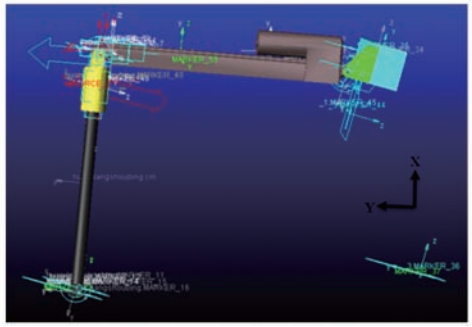

Fig. 7 Virtual proto type of tractor driver robot's gear shift mechanical arm

Assuming that the input and output shaft of the clutch is a rigid body, the dynamic model of the clutch

engagement process could be established[17].

Before the synchronization, the clutch was in the stage of sliding friction. The dynamic model can be expressed as

$$\begin{cases} J_e \dot{n}_e = T_e - T_c \\ J_c \dot{n}_c = T_c - T_r \end{cases} \tag{20}$$

In such equation set, J_e is active shaft inertia of clutch, J_c is driven shaft inertia of clutch which includes the equivalent rotational inertia of the transmission, tire and vehicle, n_e is not only the active shaft rotate speed of clutch but also the engine speed, n_c is driven shaft rotate speed of clutch, T_e is not only the active shaft torque of clutch but also the torque of engine output, T_c is sliding force torque of clutch, T_r is driven shaft resistance torque of clutch.

T_e is a nonlinear function of the throttle opening α and the engine speed n_e.

$$T_e = T_e(\alpha, n_e) \tag{21}$$

T_r is a function of the overall mass of tractor M, road's rolling resistance coefficient f, first gear speed ratio i_1, main reducer speed ratio i_0, tire's radius R.

$$T_r = T_r(M, f, i_0, i_1, R) \tag{22}$$

After synchronization, $n_e = n_c$. The dynamic equation can be interpreted as

$$(J_e + J_c)\dot{n}_c = T_e - T_r \tag{23}$$

The movement of the manipulator is simulated in two kinds of states-with clutch operation or without clutch operation. The curves of the velocity and acceleration of the mechanical arm are shown in Fig. 8. From the emulational curves and kinetic curves, some rules can be attained: the action of clutch could affect the magnitude and synchronization time of gear meshing force; compared some parameters without clutch operation, the jitter of the movement speed and the acceleration of the actuator are smaller and the smoothness of the curve is better with clutch operation. Owing to the movement of joystick in sleeve is nonlinear and the simplification of physical quantities when the dynamic model was established, there was a certain error between the the curve of calculation and simulation at the momoent of initial shifting and entering into position. The simulation results verified the correctness of the dynamic formula which provided evidence for the optimal design of the robot.

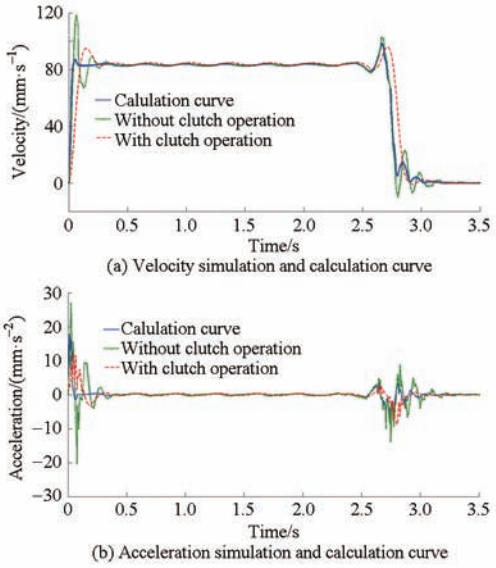

Fig. 8 Dynamics simulation curves of manipulator

3 Optimization design and motion simulation analysis of gear shift mechanical arm

In order to improve the smoothness of shifting, the optimization design of the mechanical arm was carried out. By considering the optimization design variates, constraint conditions and objective functions in this paper, ADAMS was used to set model of mechanical arm. X, Y coordinates of the two ends of the manipulator were set as design variates and then optimizing the design variates[18]. Since the design variates of this paper were less, all the design variates can be considered at the same time. By simulating and analyzing, the optimal results can be obtained. ADAMS was used to establish a measure to measure the relative movement speed of the end of the joystick and the sleeve. In order to ensure the best performance of the mechanical arm, the absolute value of terminal actuator's minimum jitter speed was set as the optimal object[19].

The function of optimal object can be expressed as

$$f(X) = \min \{ |v| \} \tag{24}$$

The length of the terminal actuator's sleeve is 80 mm. In order to prevent the shifting lever seperate from sleeve, the displacement between the joystick and the sleeve was set to less than 50 mm. Writing performance function and selecting following variates: D_1, the X coordinates of the front end of the mechanical arm; D_2, the Y coordinates of the front end of the mechanical arm; D_3, the X coordinates of the end of the mechanical arm; D_4, the Y coordinates of the end of the mechanical arm. The optimization

calculation was carried out by applying sequential quadratic programming method (forward difference)[20]. Parameters before and after optimization were shown in Tab. 2.

Tab. 2 Parameter values before and after optimization

Parameters	D_1	D_2	D_3	D_4
Initial value/mm	218.93	390.01	0.09	389.74
Optimized value/mm	220.15	392.80	0.16	393.25
Rate/%	0.58	0.72	77.78	0.90

According to Tab. 2 and the distance formula between two points, we can attain

$$S = \sqrt{(D_1 - D_3)^2 + (D_2 - D_4)^2} \qquad (25)$$

From the formula, researchers can get that the length of the mechanical arm S is about 220.0 mm and the height of mechanical arm's end is about 393.25 mm.

The target function curve before and after optimization are shown as Fig. 9a. The displacement and acceleration curves are shown as Figs. 9b, 9c respectively. The minium speed is shown as Fig. 10. From the results of the simulation analysis, the design variates have a great influence on the objective function. Before optimizating, the jitter was larger when sleeve moved on shifting lever. The displacement changes were also larger which can reach 40.2 mm. Acceleration can reach 270.01 mm/s^2 at 2.3 s. From above analysis, the stability of shifting was poor. After optimization, the jitter was reduced obviously. The maximum displacement of the joystick was no more than 20 mm. The acceleration had no big impact change which ensured the smoothness of shifting. From Fig. 10, a finding can be declared that after there times iterative computation, ADAMS finds an optimal solution. This optimal solution reduces the target function from 10.86 mm/s to 7.80 mm/s, whichis reduced by 28.18%, and generates a new model automatically. The average value and peak value of displacement, velocity and acceleration before and after optimization are shown in Tab. 3.

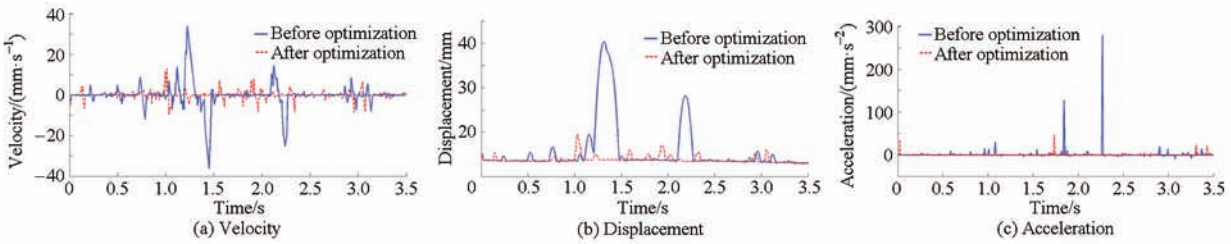

Fig. 9 Dynamic simulation results of manipulator before and after optimization

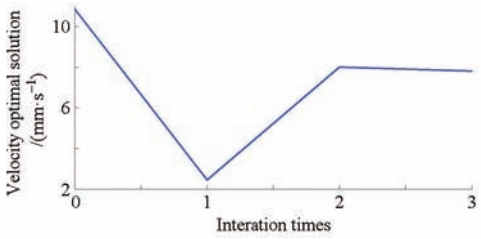

Fig. 10 Optimal solution of iterative process

Tab. 3 Average value and peak value of displacement, velocity and acceleration before and after optimization

Parameter	Displacement/ mm		Velocity/ (mm·s^{-1})		Acceleration/ (mm·s^{-2})	
	Average	Peak	Average	Peak	Average	Peak
Before optimization	19.86	40.85	10.86	35.57	12.20	272.4
After optimization	10.02	16.25	7.80	12.01	5.85	49.95
Rate/%	49.55	60.22	28.18	66.24	52.05	81.66

4 Prototype experiment of gear shift mechanical arm

According to the optimized parameters, the principle prototype of a tractor robot driver was developed. The shifting experiments were carried out on the tractor—JINMA 300E. The tractor robot driver was installed on a tractor as Fig. 11 shown.

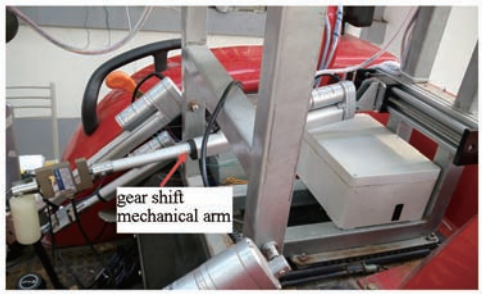

Fig. 11 Experimental tested tractor mounted with gear shift mechanical arm

The experiments were carried out under the static state and the driving state in the tractor respectively. In the process of shifting, the tractor robot driver used clutch mechanical leg to put clutch pedal to the end. Then the gear shift mechanical arm will shift gear lever

from neutral to high gear. Finally, the clutch mechanical leg was recovered, so as to release the clutch pedal and finish a shifting action. From the high gear to the low gear, the mechanical clutch leg would carry on two separation of the clutch and then use the mechanical arm to shift. Any gear in the experiment's tractor had to return to neutral gear lever. Static state experiments do not coordinate with the mechanical accelerator leg of the robot motion. The gear neutral regression experimetal curves from the rest gears to neutral gear and from the neutral gears to rest gears are shown in Fig. 12a. In about 0.8 s, when the sleeve of mechanical arm drived the joystick to move, the shifting force which was under the influence of gear meshing force and friction self-locking device was beginning to rise and reach the peak graduatelly. When the tractor was at the static state, the time for the mechanical arm shifting from the low to high gear was about 1.8 s, from high to low gear was about 2 s. Driving state experiments required the cooperatation of the mechanical throttle leg and mechanical clutch leg. The curve of shifting force experiment was shown in Fig. 12b. At about 1 s, the shifting force began to rise. Due to the vibration of the tractor, the shifting force of the mechanical arm was slightly larger than that of the tractor at static state. However, the trends of shifting force were same as that of static state. The shifting time from low to high gear and high to low gear was about 2.1 s. From Fig. 12, the mechanical arm can provide sufficient torque to control the shifting of the joystick in different gears. When the selecting gear position was fixed, the shifting operation of the mechanical arm was divided into two kinds of motion-push and pull. Under the condition that the peak value of the shifting force and the entry position of the joystick were not fixed, the mechanical arm can control the joystick to complete the shifting operation. The repeatability is good. When the joystick was in position, the proper control method was adopted to make the end of the mechanical arm to move fixed distance. Free movement of the end of the joystick in the sleeve can simulate the driver's release action after completing shifting gear. At this point, the force signal detected by the force sensor is 0. The flexible design of the end of the sleeve made the shifting process had smooth performance just like a human hand. The feasibility and rationality of the design of the mechanical arm is verified by the experiments.

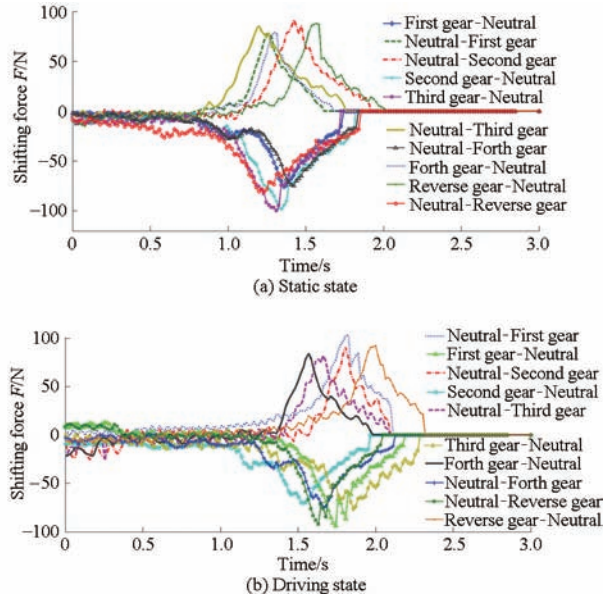

Fig. 12 Shift test result of the gear shift mechanical arm

5 Conclusion

(1) This paper analyzes the problem of controlling small tractor's shifting mechanism, and researches on the shifting resistance. Respect to the character that the gearbox shifting resistance in the four-wheel minitype agricultural tractor is time-varying and nonlinear, this paper designed a novel gear shift mechanical arm for tractor robot driver. The working principle and structure design of the mechanical arm were described in detail; using D – H method to provide the normal and inverse kinematics solutions of the mechanical arm; simplifying the structure of the mechanical arm; applying Lagrange dynamics equation to establish the mechanical kinetic equation; the correctness of the dynamic model was verified by simulation.

(2) ADAMS was applied to do kinematic and dynamic simulation. In order to guarantee the smoothness of shifting, the distance between the terminal of the manipulator's actuator and the shift lever of the tractor was set to less than 50 mm. The absolute value of terminal actuator's minimum jitter speed during shifting was optimized as the objective function. The target function was optimal when the length of shift manipulator is 220.0 mm and the height of the terminal was 393.25 mm. After optimization, the fluctuation of jitter speed was 28.18% less than

before. The rate of change of average displacement and acceleration were 49.55% and 52.05%. At the same time, the changing rate of peak value of the displacement, velocity and acceleration were 60.22%, 66.24% and 81.66% respectively. After that optimization, the movement of mechanical arm is stable and smooth.

(3)Through the experiment on gear shift mechanical arm, this paper verified that the gear shift mechanical arm can realize the goal to shift different gears smoothly with good reproducibility. In addition, when the shifting lever entered into position, the gear shift mechanical arm can complete some complicated actions such as releasing of tractor's driver by applying suitable method. Thus, the gear shift mechanical arm has excellent engineering and application value.

References

[1] Rahman A, Yahya A. Performance investigation of an advanced tracked prime mover on the low bearing soil [J]. Journal of Terramechanics, 2013, 50(4): 233 – 244.

[2] Keicher R, Seufert H. Automatic guidance for agricultural vehicles in Europe [J]. Computers and Electronics in Agriculture, 2000, 25(1): 169 – 194.

[3] Vilca J, Adouane L, Mezouar Y. A novel safe and flexible control strategy based on target reaching for the navigation of urban vehicles [J]. Robotics and Autonomous Systems, 2015, 70: 215 – 226.

[4] Wang Guangming, Zhu Sihong, Shi Lixin, et al. Control and interaction system for tractor hydro-mechanical CVT [J]. Transactions of the Chinese Society for Agricultural Machinery, 2015, 46(6): 1 – 7. (in Chinese)

[5] Han Keli, Zhu Zhongxiang, Mao Enrong, et al. Joint control method of speed and heading of navigation tractor based on optimal control[J]. Transactions of the Chinese Society for Agricultural Machinery, 2013, 44(2): 165 – 170. (in Chinese)

[6] Shoval S, Zyburt J P, Grimaudo D W. Robot driver for guidance of automatic durability road (ADR) test vehicles[C]// 1998 IEEE International Conference on Robotics and Automation, 1998, 2: 1767 – 1772.

[7] Chen Gang, Zhang Weigong, Gong Zongyang, et al. Coordinated control of multiple manipulators for vehicle robot driver[J]. Chinese Journal of Scientific Instrument, 2009, 30(9): 1836 – 1840. (in Chinese)

[8] Zhang Weigong, Chen Xiaobing. Key technologies of vehicle robot driver[J]. Journal of Jiangsu University: Natural Science Edition, 2005, 26(1): 20 – 23. (in Chinese)

[9] Matsumura T, Ichikawa S, Katsu F, et al. The development of a controller confirmation system for automatic transmissions and its applications[C]// Control Applications, 2004. Proceedings of the 2004 IEEE International Conference on. IEEE, 2004, 2: 1415 – 1419.

[10] Chen Gang, Zhang Weigong, Chang Siqin. Shift control method of vehicle robot driver based on fuzzy neural network[J]. Transactions of the Chinese Society for Agricultural Machinery, 2011, 42(6): 6 – 11. (in Chinese)

[11] Jin Jingsu, Li Yongjun, Xu Haiping. The application of synchronizer in Jiangsu 750 tractor transmission[J]. Wireless Internet Technolog, 2015(7): 138 – 139. (in Chinese)

[12] Zhou Jiliang. Structure and spectrum of tractor transmission[J]. Transactions of the Chinese Society for Agricultural Machinery, 1979, 10(2): 47 – 63. (in Chinese)

[13] He B, Han L, Wang Y, et al. Kinematics analysis and numerical simulation of a manipulator based on virtual prototyping[J]. The International Journal of Advanced Manufacturing Technology, 2014, 71(5 – 8): 943 – 963.

[14] Udriste C, Tevy I. Multi-time Euler-Lagrange dynamics [C]// Proceedings of the 7th WSEAS International Conference on Systems Theory and Scientific Computation (ISTASC'07), Vouliagmeni Beach, Athens, Greece, 2007: 66 – 71.

[15] Liu Y C, Chopra N. Controlled synchronization of heterogeneous robotic manipulators in the task space [J]. IEEE Transactions on Robotics, 2012, 28(1): 268 – 275.

[16] Heidarbeigi K, Ahmadi H, Omid M, et al. Evolving an artificial neural network classifier for condition monitoring of massy ferguson tractor gearbox [J]. International Journal of Applied Engineering Research, 2010, 5(12): 2097 – 2107.

[17] Zhang J, Chen L, Xi G. System dynamic modelling and adaptive optimal control for automatic clutch engagement of vehicles [J]. Proceedings of the Institute of Mechanical Engineers Part D: Journal of Automobile Engineering (S0954 – 4070), 2002, 216(12): 983 – 991.

[18] Chen Yuxiang. Simulation analysis on the shifting performance of mechanical transmission based on virtual prototype technology [D]. Guangzhou: South China University of Technology, 2012. (in Chinese)

[19] Xu Xiang, Hou Liya, Huang Xinyan, et al. Design and research of a wearable robot for upper limbs rehabilitation based on exoskeleton[J]. Robot, 2014, 36(2): 147 – 155. (in Chinese)

[20] Qin Dongcheng, Wang Lixia, Liu Zhuli, et al. A study on SQP method application for large-scale structural optimization design[J]. Henan Science, 2006, 24(3): 431 – 433. (in Chinese)

doi:10.6041/j.issn.1000-1298.2016.01.006

拖拉机驾驶机器人换挡机械手运动分析

卢　伟[1,2]　陈　浩[1]　王　玲[1]　赵贤林[1]　章永年[1]

(1.南京农业大学工学院,南京 210031;2.远程测控技术江苏省重点实验室,南京 210096)

摘要:针对小型四轮农用拖拉机变速箱换挡阻力呈现时变、非线性特性,且换挡后需要松开换挡杆的特殊要求,设计了拖拉机驾驶机器人换挡机械手,该机械手为关节型结构,采用 D-H 方法建立机械手坐标变换矩阵,对机械手进行运动学分析,并通过拉格朗日动力学方程建立简化机械手的动力学模型。利用 SolidWorks 建立换挡机械手虚拟样机模型,并采用多体动力学仿真软件 ADAMS 进行运动学和动力学仿真;为保证换挡平顺性,设置机械手末端执行器与拖拉机变速杆端部间位移小于 50 mm 为约束条件,将换挡过程中末端执行器抖动速度绝对值最小作为目标函数进行参数优化,当换挡机械手长度为 220.0 mm、末端高度为 393.25 mm 时目标函数最优,此时机械手末端执行器抖动速度平均值较优化前减小 28.18%,位移和加速度平均值变化率分别为 49.55% 和 52.05%,位移、速度和加速度的峰值变化率分别为 60.22%、66.24% 和 81.66%,通过仿真初步验证了所提机械手参数优化及所建模型的合理性和科学性。最后,在 JINMA 300E 型拖拉机上对优化后的换挡机械手进行实验研究,实验结果表明机械手可实现不同挡位的换挡动作,平顺性好,并可模拟拖拉机驾驶员换挡完成后对变速杆的松手动作,有良好的工程和应用价值。

关键词:拖拉机;驾驶机器人;换挡;运动仿真;参数优化

中图分类号:TP242.3　　**文献标识码**:A　　**文章编号**:1000-1298(2016)01-0037-08

Motion Analysis of Tractor Robot Driver's Gear Shift Mechanical Arm

Lu Wei[1,2]　Chen Hao[1]　Wang Ling[1]　Zhao Xianlin[1]　Zhang Yongnian[1]

(1. *College of Engineering*, *Nanjing Agricultural University*, *Nanjing* 210031, *China*

2. *Key Laboratory of Remote Control and Measurement Technology in Jiangsu Province*, *Nanjing* 210096, *China*)

Abstract: Respect to the character that the gearbox shifting resistance exist in the four-wheel minitype agricultural tractor is time-varying and nonlinear and the special requirement that the gear shift lever has to be released after shifting, this paper designed a novel gear shift mechanical arm for tractor robot driver. This manipulator is joint type. According to the manipulator's operating characteristic, this paper applied D-H method to establish the coordinate transformation matrix. Based on the kinematics analysis on the manipulator, Lagrange equation was used to simplify kinetic model of the manipulator. SolidWorks and ADAMS were applied to establish the virtual prototype model of the manipulator and to do kinematic and dynamic simulation respectively. In order to guarantee the smoothness of shift, the distance between the terminal of the manipulator's actuator and the gear shift lever of the tractor was set to less than 50 mm. The absolute value of terminal actuator's minimum jitter speed during shift was optimized as the objective function. The target function is optimal when the length of shift manipulator is 220.0 mm and the height of the terminal is 393.25 mm. After optimization, the jitter speed fluctuation is 28.18% less than before. The rate of change of average displacement and average acceleration are 49.55% and 52.05%. At the same time, the peak value of the displacement, velocity and acceleration are 60.22%,

收稿日期:2015-07-20　修回日期:2015-10-08

基金项目:国家自然科学基金青年基金项目(51405239)、江苏省自然科学基金青年基金项目(BK20130696)、中央高校基本科研业务费专项资金项目(KYZ201427)和远程测控技术江苏省重点实验室开放基金项目(YCCK201501)

作者简介:卢伟(1978—),男,副教授,博士,主要从事机器人传感与控制、无损检测及微弱信号处理研究,E-mail:njaurobot@njau.edu.cn

66.24% and 81.66%, respectively. Through the simulation, the optimization of the parameters of the manipulator, the rationality and the scientificity of the model are verified. Finally, through the experiment on gear shift mechanical arm on JINMA 300E tractor, the result shows that the gear mechanical arm can realize the goal to shift different gears smoothly. In addition, the design of the gear mechanical arm can complete some complicated actions of tractor's driver. Thus, the gear shift mechanical arm has excellent engineering and application value.

Key words: tractor; robot driver; gear shift; motion simulation; parameter optimization

引言

我国拖拉机的自动化和智能化发展相对滞后,目前学者主要研究基于多传感器智能控制的农用车辆自动驾驶技术,并取得了很多有价值的成果,例如北海道大学、伊利诺伊大学、爱媛大学、华南农业大学、中国农业大学、南京农业大学等研究过农用拖拉机无人驾驶[1-3],涉及拖拉机执行机构的改造及驾驶控制等。此外,Deere、CNH、AGCO、Kubota、芬特等公司的部分产品也具有无人驾驶功能[4-5]。但智能拖拉机需要对拖拉机进行二次改造,其成本较高,而且拖拉机一旦损坏,安装在上面的智能设备很难移植到其他拖拉机;相比较而言,驾驶机器人技术的发展为解决农业智能化问题提供了契机,当下驾驶机器人替代人类驾驶员完成汽车驾驶操作已经成为汽车测试行业的发展趋势,驾驶机器人已经发展成一个集成式系统,由换挡机械手、离合踏板机械腿、制动踏板机械腿、油门踏板机械腿子系统构成,每一个执行机构都可以单独安装并完成相应的测试实验。汽车驾驶机器人已经成为近代汽车实验中必不可少的智能化装置[6]。现在国外已研制出纯电驱动的驾驶机器人,并可以代替驾驶员进行道路实验,如日本 HORIBO、Nissan Motor、AUTOMAX 公司、德国 SCHENCK 公司、英国 MIRA 公司,而国内相关的研究还比较少[7-10],国内外的各大汽车驾驶机器人基本被国外公司的产品占据。

由于拖拉机的特殊机械结构,将驾驶机器人技术应用到四轮农用拖拉机目前鲜有报道,研究通用性强、高性能的拖拉机驾驶机器人可以对传统农用拖拉机进行无损、智能化升级,具有重要的现实意义和科学价值。拖拉机因其价格低廉,拉力巨大,因此结构与汽车差异显著,能够实现自动换挡的拖拉机驾驶机器人,其技术难点之一就是小型拖拉机手动变速箱操控非常困难,且换挡后必须松开换挡杆。本文针对小型四轮农用拖拉机智能化升级中变速箱自动换挡的技术难点,设计换挡机械手,并进行理论和实验研究。

1 拖拉机驾驶机器人换挡机械手设计

1.1 拖拉机驾驶机器人换挡机械手需求参数分析

目前应用较广泛的中大型拖拉机大多采用同步器换挡,而小型拖拉机大多采用机械手动式齿轮变速箱进行换挡[11-12]。换挡过程中拨叉通过拨动滑动齿轮,使其与相关齿轮啮合或分离,变速杆用球头作为支撑,保证变速杆下端不仅能前、后运动,而且可左、右移动,变速杆前后运动时带动拨叉使滑动齿轮移动,滑动齿轮入位后,应能将其锁定,变速杆左右移动时,其下端在拨叉槽内移动,选挡阻力小且较平顺。

同汽车变速箱相比,小型拖拉机变速箱中滑动齿轮较大、齿轮啮合力、不同步撞击等导致拖拉机变速箱换挡阻力较大,且呈现非线性特征,换挡时拨叉拨动滑动齿轮,滑动齿轮通过齿形端面与轴上的齿轮啮合,从而将发动机的主动力传递到相应轴上,滑动齿轮与轴上齿轮啮合后,需要松开变速杆,保证换挡稳定性及延长齿轮寿命。换挡机构如图 1 所示。

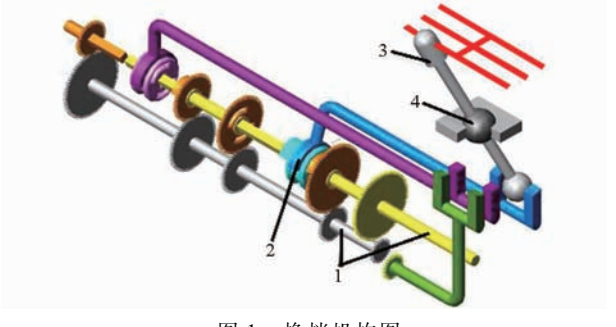

图 1 换挡机构图

Fig. 1 Shifting mechanism

1. 轴 2. 拨叉 3. 变速杆 4. 球支撑

在拖拉机变速杆工作空间上方水平固定步进电动机驱动的 *XY* 十字电动直线滑台,滑台工作平面通过力传感器与拖拉机变速杆固定连接,测量拖拉机实际换挡距离和换挡阻力,通过测量可知,拖拉机变速杆选挡时端部在 *X* 方向运动范围约 200 mm,在 *Y* 方向运动范围约 85 mm。

将拖拉机发动并将主动轮悬空,由空挡换到其他挡位时的换挡阻力如图 2 所示。在变速杆入位前

时刻换挡阻力达到峰值，约为 80 N，且换挡阻力具有时变、非线性等显著特征。

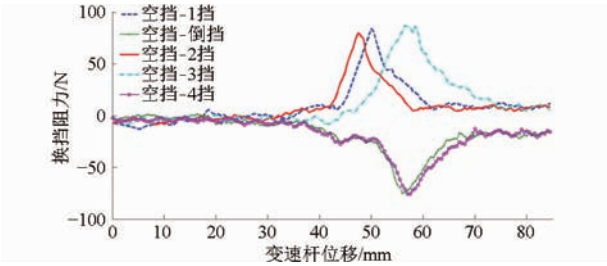

图 2　换挡阻力曲线

Fig. 2　Curves of shifting resistance

1.2　拖拉机驾驶机器人换挡机械手结构设计

根据上述分析和机械手换挡参数需求，拖拉机驾驶机器人的机构设计如图 3 所示，该机械手主要由 X 方向执行机构和 Y 方向执行机构构成。其中 X 方向执行机构选用CY－42YT200 型直线光杆导轨滑台，并配有 42H4812 型两相混合式步进电动机，转矩为 0.5 N·m，精度为 0.1 mm；Y 方向执行机构采用带增益码盘的电动推杆，行程为 300 mm，推力为 250N。X 方向和 Y 方向机构通过连接件相连，X 方向滑台可带动 Y 方向执行机构到达拖拉机变速杆任一选挡位并精确固定，Y 方向电动推杆可控制变速杆到达任一换挡位，从而实现机械手 2 个方向的运动解耦。机械手前端带有力传感器用于检测换挡过程中的推拉力，末端抱紧装置为塑性材质的套筒，套筒将变速杆端部套住，套筒直径略大于变速杆直径，使变速杆入位后可在套筒内做小幅度自由运动，近似模拟驾驶员换挡完成后的松手动作，保证拖拉机换挡器内部基本无摩擦。

图 3　拖拉机驾驶机器人换挡机械手三维模型

Fig. 3　Three-dimensional model of tractor driver robot's gear shift mechanical arm

1. 步进电动机　2. 滑台　3. 直线导轨　4. 连接件　5. 电动推杆　6. 力传感器　7. 套筒(抱紧装置)

2　机械手运动学与动力学分析

2.1　机械手运动学正解

将本文机械手等效成关节型机械手，在关节处固接一个坐标系，并通过 D－H 方法[13]来描述这些坐标系之间的相对位置和姿态。为了减少计算量，进行等效处理，共给出 4 个坐标系，机械手坐标系简图如图 4 所示，其中 $O_0X_0Y_0Z_0$ 为基坐标系，为滑台在直线导轨选挡位置的坐标系，l_2 为滑台 Y 方向移动距离，$O_2X_2Y_2Z_2$ 为 $O_1X_1Y_1Z_1$ 旋转角度 θ_2 后的坐标系，d_3 为机械手 X 方向的移动距离，$O_3X_3Y_3Z_3$ 为固接于机械手末端执行器上用于表述机械手位姿的坐标系。

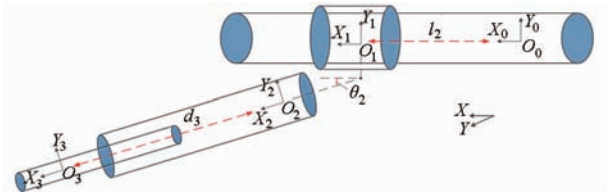

图 4　机械手坐标系简图

Fig. 4　Coordinate system of mechanical arm

根据 D－H 方法，对于运动链中的末端连杆，其参数习惯设定为 0，由图 4 可得机械手的连杆参数表如表 1 所示。

表 1　机械手连杆参数

Tab. 1　Link parameters of mechanical arm

i	α_{i-1}	a_{i-1}	d_i	θ_i
1	0	0	0	0
2	0	0	l_2	θ_2
3	0	d_3	0	0

将上述参数代入变换矩阵 ${}_{i}^{i-1}\boldsymbol{T}$ 的一般表达式

$$ {}_{i}^{i-1}\boldsymbol{T}=\begin{bmatrix} c\theta_i & -s\theta_i & 0 & a_{i-1} \\ s\theta_i c\alpha_{i-1} & c\theta_i c\alpha_{i-1} & -s\alpha_{i-1} & -s\alpha_{i-1}d_i \\ s\theta_i s\alpha_{i-1} & c\theta_i s\alpha_{i-1} & c\alpha_{i-1} & c\alpha_{i-1}d_i \\ 0 & 0 & 0 & 1 \end{bmatrix} \tag{1} $$

可得

$$ \begin{cases} {}_{1}^{0}\boldsymbol{T}=\begin{bmatrix} 1 & 0 & 0 & 0 \\ 0 & 1 & 0 & 0 \\ 0 & 0 & 1 & 0 \\ 0 & 0 & 0 & 1 \end{bmatrix} \\ {}_{2}^{1}\boldsymbol{T}=\begin{bmatrix} c\theta_2 & -s\theta_2 & 0 & 0 \\ s\theta_2 & c\theta_2 & 0 & 0 \\ 0 & 0 & 1 & l_2 \\ 0 & 0 & 0 & 1 \end{bmatrix} \\ {}_{3}^{2}\boldsymbol{T}=\begin{bmatrix} 1 & 0 & 0 & d_3 \\ 0 & 1 & 0 & 0 \\ 0 & 0 & 1 & 0 \\ 0 & 0 & 0 & 1 \end{bmatrix} \end{cases} \tag{2} $$

$$ {}_{3}^{0}\boldsymbol{T}={}_{1}^{0}\boldsymbol{T}_{2}^{1}\boldsymbol{T}_{3}^{2}\boldsymbol{T}=\begin{bmatrix} c\theta_2 & -s\theta_2 & 0 & d_3c\theta_2 \\ s\theta_2 & c\theta_2 & 0 & d_3s\theta_2 \\ 0 & 0 & 1 & l_2 \\ 0 & 0 & 0 & 1 \end{bmatrix} \tag{3} $$

式中，$s\theta_2$ 表示 $\sin\theta_2$，$c\theta_2$ 表示 $\cos\theta_2$。

运动学方程表示了机械手末端执行器的空间位置和方向矢量,以及其位姿同各构件参数之间的变换关系。

2.2 机械手运动学逆解

运动逆解要求由末端执行器的笛卡尔空间相对于基坐标系变换,通过已确定的量求出关节转角 θ_2,已知可确定目标点的变换矩阵 ${}_3^0\boldsymbol{T}$ 为

$$ {}_3^0\boldsymbol{T}=\begin{bmatrix} c\theta_2 & -s\theta_2 & 0 & x \\ s\theta_2 & c\theta_2 & 0 & y \\ 0 & 0 & 1 & l_2 \\ 0 & 0 & 0 & 1 \end{bmatrix} \tag{4}$$

故可得

$$\tan\theta_2=\frac{y}{x} \tag{5}$$

于是

$$\theta_2=\arctan\frac{y}{x} \tag{6}$$

对换挡机械手进行运动学分析,变速杆工作空间投影和机械手工作空间投影如图 5 所示,变速杆选挡方向和换挡方向的运动投影为 -100 ~ 100 mm 和 0 ~ 85 mm,投影面积为 17 000 mm^2,机械手工作空间在 X 方向和 Y 方向的水平投影分别为 -120 ~ 120 mm 和 0 ~ 100 mm,投影面积为 24 000 mm^2,由图 5 可知,机械手工作空间完全覆盖了拖拉机变速杆的工作空间,能够满足拖拉机换挡要求,仿真验证了机械手结构设计和运动学算法的科学性、合理性。

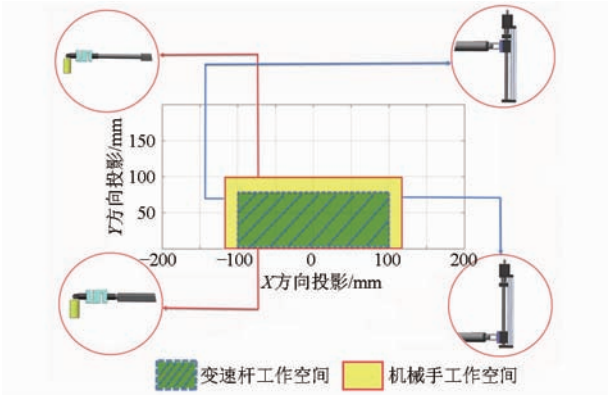

图 5 换挡机械手工作空间

Fig. 5 Working space of gear shift mechanical arm

2.3 机械手动力学分析

拉格朗日动力学公式[14]给出了一种从标量函数推导动力学方程的方法,该标量函数为拉格朗日函数,本文中,机械手的拉格朗日函数表示为

$$L(\boldsymbol{\Theta},\dot{\boldsymbol{\Theta}})=k(\boldsymbol{\Theta},\dot{\boldsymbol{\Theta}})-u(\boldsymbol{\Theta}) \tag{7}$$

则机械手的运动方程为[15]

$$\frac{\mathrm{d}}{\mathrm{d}t}\frac{\partial L}{\partial\dot{\boldsymbol{\Theta}}}-\frac{\partial L}{\partial\boldsymbol{\Theta}}=\boldsymbol{\tau} \tag{8}$$

由式(7)和式(8)可得

$$\frac{\mathrm{d}}{\mathrm{d}t}\frac{\partial k}{\partial\dot{\boldsymbol{\Theta}}}-\frac{\partial k}{\partial\boldsymbol{\Theta}}+\frac{\partial u}{\partial\boldsymbol{\Theta}}=\boldsymbol{\tau} \tag{9}$$

式中 $k(\boldsymbol{\Theta},\dot{\boldsymbol{\Theta}})$——机械手动能

$u(\boldsymbol{\Theta})$——机械手势能

$\boldsymbol{\tau}$ ——$n\times1$ 维的驱动力矢量

$\boldsymbol{\Theta}$——关节位置

采用集中质量法将机械手 Y 方向执行机构简化为图 6 所示,机械手的动力自由度为 2,其后端的质量为 m_1,伸出端、力传感器及抱紧装置的质量和为 m_2,机械手后端的质心与关节的轴线相距 l_1,伸出端、力传感器及抱紧装置的质心与关节轴线的距离为变量 d_2。

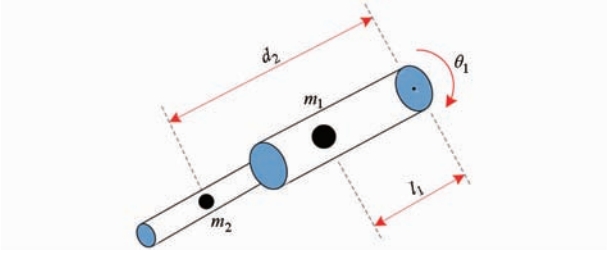

图 6 机械手 Y 方向的运动简图

Fig. 6 Motion diagram of mechanical arm in Y direction

机械手后端和伸出端的惯性张量分别为

$$\begin{cases} {}^{C_1}\boldsymbol{I}_1=\begin{bmatrix} I_{xx1} & 0 & 0 \\ 0 & I_{yy1} & 0 \\ 0 & 0 & I_{zz1} \end{bmatrix} \\ {}^{C_2}\boldsymbol{I}_2=\begin{bmatrix} I_{xx2} & 0 & 0 \\ 0 & I_{yy2} & 0 \\ 0 & 0 & I_{zz2} \end{bmatrix} \end{cases} \tag{10}$$

为简化计算,将机械手近似等效为质量均匀的实体,式(10)矩阵中的各元素为

$$\begin{cases} I_{xx}=\iiint_V(y^2+z^2)\rho\mathrm{d}v \\ I_{yy}=\iiint_V(x^2+z^2)\rho\mathrm{d}v \\ I_{zz}=\iiint_V(x^2+y^2)\rho\mathrm{d}v \end{cases} \tag{11}$$

机械手后端的动能为

$$k_1=\frac{1}{2}m_1l_1^2\dot{\theta}_1^2+\frac{1}{2}I_{zz1}\dot{\theta}_1^2 \tag{12}$$

机械手伸出端、力传感器及抱紧装置的动能为

$$k_2=\frac{1}{2}m_2(d_2^2\dot{\theta}_1^2+\dot{d}_2^2)+\frac{1}{2}I_{zz2}\dot{\theta}_1^2 \tag{13}$$

由式(12)和式(13)可得总动能为

$$k(\boldsymbol{\Theta},\dot{\boldsymbol{\Theta}})=\frac{1}{2}(m_1l_1^2+I_{zz1}+I_{zz2}+m_2d_2^2)\dot{\theta}_1^2+\frac{1}{2}m_2\dot{d}_2^2 \tag{14}$$

机械手后端的势能为

$$u_1 = m_1 l_1 g\sin\theta_1 + m_1 l_1 g \tag{15}$$

机械手伸出端、力传感器及抱紧装置的势能为

$$u_2 = m_2 d_2 g\sin\theta_1 + m_2 g d_{2\max} \tag{16}$$

式中　$d_{2\max}$——末端执行器的最大运动范围

由式(12)和式(13)得总势能为

$$u(\boldsymbol{\Theta}) = (m_1 l_1 + m_2 d_2) g\sin\theta_1 + m_1 l_1 g + m_2 g d_{2\max} \tag{17}$$

求偏导数代入式(9)可得机械手最终的动力学方程为

$$\boldsymbol{\tau}_1 = (m_1 l_1^2 + I_{zz1} + I_{zz2} + m_2 d_2^2)\ddot{\theta}_1 + 2m_2 d_2 \dot{\theta}_1 \dot{d}_2 + (m_1 l_1 + m_2 d_2) g\cos\theta_1 \tag{18}$$

$$\boldsymbol{\tau}_2 = m_2 \ddot{d}_2 - m_2 d_2 \dot{\theta}_1^2 + m_2 g\sin\theta_1 \tag{19}$$

在 SolidWorks 中建立换挡机械手装配体虚拟样机模型，导入到 ADAMS 中，如图 7 所示，机械手模型中各个零件的特性参数根据物理样机实际材料设置，根据各个关节运动副情况施加相关的运动约束，为验证换挡机械手动力学模型的正确性，仿真过程同时考虑变速箱齿轮啮合力和自锁装置阻力。根据拖拉机换挡实验得知，对于手动变速器滑动齿轮换挡，必须配以离合器的操作才能完成，特别是在高挡换抵挡时，为避免齿轮发生冲撞而损坏，需要进行两次分离离合器才能挂上挡，并且变速杆在入位时刻阻力会明显下降[16]，在 ADAMS 仿真过程中创建传感器，控制机械手在变速箱滑动齿轮入位后停止运动。

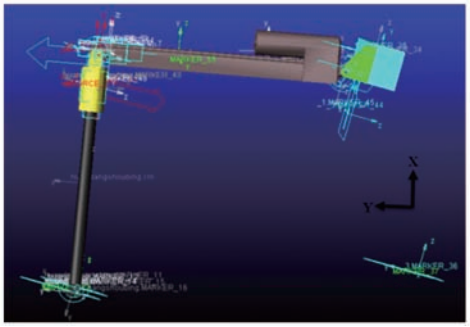

图 7　拖拉机驾驶机器人换挡机械手虚拟样机模型

Fig. 7　Virtual proto type of tractor driver robot's gear shift mechanical arm

假设离合器输入输出轴为刚体，建立离合器接合过程的动力学模型[17]。

同步之前，离合器处于滑摩阶段，其动力学模型为

$$\begin{cases} J_e \dot{n}_e = T_e - T_c \\ J_c \dot{n}_c = T_c - T_r \end{cases} \tag{20}$$

式中　J_e——离合器的主动轴惯量

J_c——离合器从动轴惯量，包括变速器、轮胎、整车的等效转动惯量

n_e——离合器主动轴转速，也是发动机转速

n_c——离合器从动轴转速

T_e——离合器主动轴动力矩，也是发动机输出扭矩

T_c——离合器滑摩扭矩

T_r——离合器从动轴阻力矩

T_e 是油门开度 α 和发动机转速 n_e 的非线性函数。

$$T_e = T_e(\alpha, n_e) \tag{21}$$

T_r 是整体拖拉机质量 M、道路滚动阻力系数 f、Ⅰ挡速比 i_1、主减速器速比 i_0、轮胎半径 R 的函数。

$$T_r = T_r(M, f, i_0, i_1, R) \tag{22}$$

同步后，$n_e = n_c$，此时动力学方程为

$$(J_e + J_c)\dot{n}_c = T_e - T_r \tag{23}$$

在有离合器操作和无离合器操作两种状态下仿真机械手的运动过程。机械手运动速度、加速度随时间的变化曲线如图 8 所示，由仿真曲线和动力学计算曲线可知：离合器的动作会直接影响到齿轮啮合力的大小和同步时间，换挡时有离合器操作与无离合器操作相比，机械手末端执行器的运动速度、加速度抖动较小，曲线的平滑性也更好，曲线的拟合程度较高。由于变速杆端部在套筒中运动呈现一定的非线性以及动力学模型建立时简化物理量，导致计算曲线和仿真曲线在换挡初始时刻和入位时刻有一定误差，仿真结果验证了动力学公式的正确性，该结果为机器人的优化设计提供了依据。

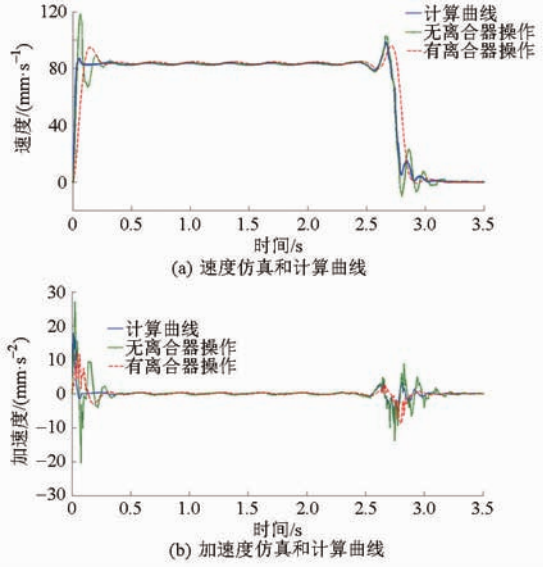

图 8　机械手动力学仿真曲线

Fig. 8　Dynamics simulation curves of manipulator

3　换挡机械手优化设计与运动仿真分析

为提高换挡平顺性，对机械手进行优化设计。

综合考虑本文的优化设计变量、约束条件及目标函数,应用 ADAMS 对机械手进行参数化建模。将机械手两端点的 X、Y 坐标一共 4 个变量作为设计变量,对其进行优化分析[18],由于本文设计变量较少,可同时考虑各个设计变量,对其进行仿真分析,得出优化结果。

采用 ADAMS 建立一个 Measure,测量变速杆端部和套筒相对运动速度,为保证机械手运动平顺性最佳,设置机械手末端执行器在变速杆上的抖动速度绝对值最小为优化目标[19],即优化目标函数为

$$f(X) = \min\{|v|\} \tag{24}$$

机械手末端执行器套筒的长度为 80 mm,换挡过程中变速杆不能脱离套筒约束,故设置约束条件为套筒距变速杆端部的位移小于 50 mm,编写功能函数,变量选择为:D_1,机械手前端点的 X 坐标值;D_2,机械手前端点的 Y 坐标值;D_3,机械手后端点的 X 坐标值;D_4,机械手后端点的 Y 坐标值。采用序列二次(向前差分)规划法[20]进行优化计算。优化前后参数如表 2 所示。

根据表 2 及两点间距离公式

$$S = \sqrt{(D_1 - D_3)^2 + (D_2 - D_4)^2} \tag{25}$$

确定了换挡机械手长度 S 约为 220.0 mm,末端高度约为 393.25 mm。

表 2 优化前后参数值

Tab. 2 Parameter values before and after optimization

参数	D_1	D_2	D_3	D_4
初值/mm	218.93	390.01	0.09	389.74
优化后/mm	220.15	392.80	0.16	393.25
变化率/%	0.58	0.72	77.78	0.90

优化前后目标函数变化曲线如图 9a 所示,位移和加速度变化曲线分别如图 9b 和 9c 所示。各次迭代过程中求解得到的最小速度如图 10 所示,从仿真分析结果可看出,设计变量对目标函数的影响很大,优化前机械手末端套筒在拖拉机变速杆上的抖动较大,位移变化较大,最大达到 40.2 mm,加速度在 2.3 s 时刻达到 270.01 mm/s^2,换挡稳定性较差;优化后抖动明显减小,变速杆在套筒内位移最大不超过 20 mm,加速度也无较大冲击变化,保证了换挡平顺性。由图 10 知,经过 3 次迭代运算,ADAMS 找到一个最优解,使得目标函数由 10.86 mm/s 减小到 7.80 mm/s,减小了 28.18%,并自动生成新的样机模型。优化前后位移、速度、加速度的峰值和平均值变化率见表 3。

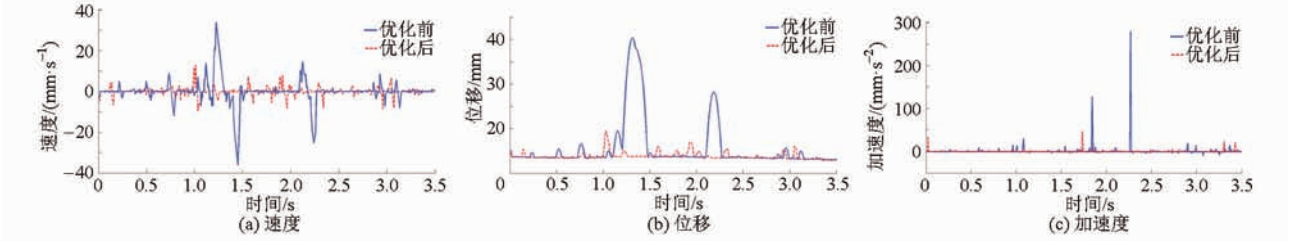

图 9 机械手优化前后的动力学仿真结果

Fig. 9 Dynamic simulation results of manipulator before and after optimization

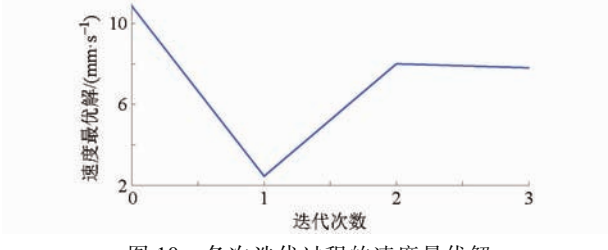

图 10 各次迭代过程的速度最优解

Fig. 10 Optimal solution of iterative process

表 3 优化前后位移、速度和加速度的对比

Tab. 3 Average value and peak value of displacement, velocity and acceleration before and after optimization

参数	位移/mm		速度/(mm·s^{-1})		加速度/(mm·s^{-2})	
	均值	峰值	均值	峰值	均值	峰值
优化前	19.86	40.85	10.86	35.57	12.20	272.37
优化后	10.02	16.25	7.80	12.01	5.85	49.95
变化率/%	49.55	60.22	28.18	66.24	52.05	81.66

4 换挡机械手样机实验

根据优化参数研制了拖拉机驾驶机器人换挡机械手的原理样机,并在 JINMA 300E 型拖拉机上进行了换挡实验,拖拉机驾驶机器人在拖拉机上的安装如图 11 所示。

分别在拖拉机静止状态和行驶状态下进行换挡实验,换挡过程中拖拉机驾驶机器人利用离合器机械腿将离合踏板踩到底,通过换挡机械手将变速杆从空挡换到高挡,然后离合器机械腿回收,放松离合踏板,完成一次换挡动作,由高挡换到低挡时,离合器机械腿进行两次分离离合器的操作,再由机械手进行换挡动作,实验用拖拉机换任一挡位时都需将变速杆回归空挡。静止状态实验不配合驾驶机器人油门机械腿的运动,由空挡到其余各挡位和由其余

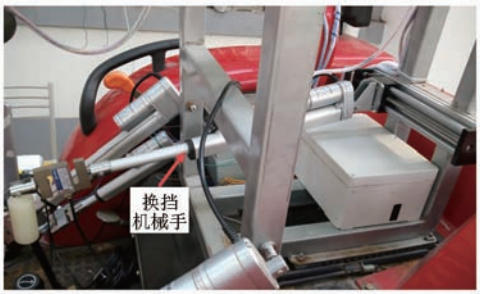

图 11　安装有换挡机械手的实验拖拉机

Fig. 11　Experimental tested tractor mounted with gear shift mechanical arm

各挡位回归空挡的换挡力实验曲线如图 12a 所示，在大约 0.8 s，当机械手末端套筒带动拖拉机变速杆运动时，在齿轮啮合力和自锁装置阻力作用下换挡力开始上升，逐渐到达峰值，拖拉机静止状态时机械手由低挡到高挡的换挡时间约为 1.8 s，从高挡到低挡的换挡时间约为 2 s。拖拉机行驶状态实验需同时配合驾驶机器人油门机械腿和离合器机械腿的运动，换挡力实验曲线如图 12b 所示，在大约 1 s 时换挡力开始上升，由于拖拉机运动时的振动，机械手换挡力较拖拉机静止时换挡力抖动略大，但换挡力趋势和拖拉机静止时保持一致，低挡到高挡、高挡到低挡的换挡时间约为 2.1 s。由图 12 可见，换挡机械手可提供足够力矩控制变速杆在不同挡位之间变换。在选挡位置固定时，机械手换挡动作分推和拉两种运动状态，在各挡位力峰值和变速杆入位点均不固定的情况下，机械手可稳定控制拖拉机变速杆完成换挡动作，重复性好，当变速杆入位后，采用合适的控制方法使机械手末端执行器回移固定距离，其端部在套筒内自由运动，模拟驾驶员换挡完成后对变速杆的松手动作，此时力传感器检测到的力信号为零，末端套筒的柔性化设计使得换挡过程具有近似人手的平顺性。实验验证了换挡机械手设计的可行性和合理性。

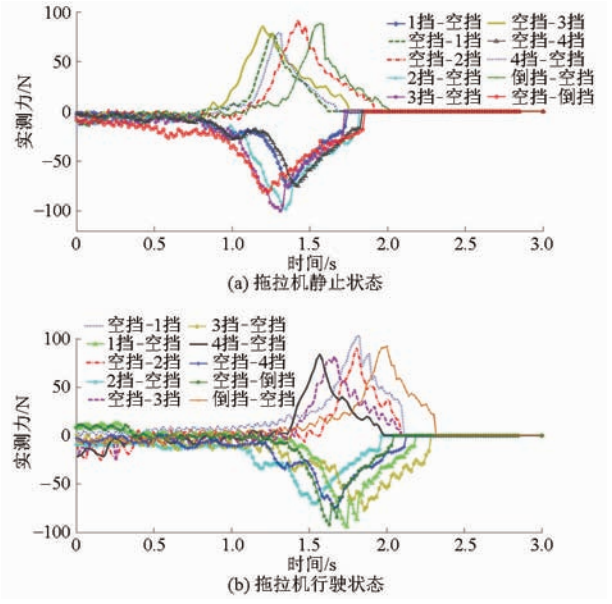

图 12　换挡机械手换挡实验结果

Fig. 12　Shift test result of gear shift mechanical arm

5　结论

（1）对小型拖拉机换挡机构换挡操控难的问题进行了剖析，并进行换挡阻力的测试研究；针对小型拖拉机变速箱的特殊性及换挡阻力呈现时变、非线性等特征，提出一种拖拉机驾驶机器人换挡机械手，详述了机械手的工作原理和结构设计，采用 D－H 方法给出机械手运动学正解和逆解，并将机械手结构简化，采用拉格朗日动力学公式建立机械手动力学方程，通过仿真验证了动力学模型的正确性。

（2）通过 ADAMS 对机械手进行运动仿真，设置机械手末端执行器与拖拉机变速杆端部间位移小于 50 mm 为约束条件，相对速度绝对值最小作为目标函数进行参数优化，优化结果表明当换挡机械手长度为 220.0 mm、末端高度为 393.25 mm 时目标函数达到最优，变化率为 28.18%，同时，位移和加速度平均值变化率分别为 49.55% 和 52.05%，位移、速度和加速度的峰值变化率分别为 60.22%、66.24% 和 81.66%，优化后机械手运动平稳，运动平顺性好。

（3）通过实验验证了换挡机械手可实现拖拉机变速杆不同挡位的换挡动作，重复性好；当变速杆入位后，采用合适的控制方法控制机械手回移能够有效模拟人工换挡后的松手动作，具有良好的工程和应用价值。

参　考　文　献

1　Rahman A, Yahya A. Performance investigation of an advanced tracked prime mover on the low bearing soil[J]. Journal of Terramechanics, 2013, 50(4): 233－244.

2　Keicher R, Seufert H. Automatic guidance for agricultural vehicles in Europe[J]. Computers and Electronics in Agriculture, 2000, 25(1): 169－194.

3　Vilca J, Adouane L, Mezouar Y. A novel safe and flexible control strategy based on target reaching for the navigation of urban vehicles[J]. Robotics and Autonomous Systems, 2015, 70: 215－226.

4　王光明，朱思洪，史立新，等. 拖拉机液压机械无级变速箱控制与交互系统[J]. 农业机械学报，2015，46(6)：1－7.

Wang Guangming, Zhu Sihong, Shi Lixin, et al. Control and interaction system for tractor hydro-mechanical CVT[J]. Transactions of the Chinese Society for Agricultural Machinery, 2015, 46(6): 1 - 7. (in Chinese)

5 韩科立, 朱忠祥, 毛恩荣, 等. 基于最优控制的导航拖拉机速度与航向联合控制方法[J]. 农业机械学报, 2013, 44(2): 165 - 170.
Han Keli, Zhu Zhongxiang, Mao Enrong, et al. Joint control method of speed and heading of navigation tractor based on optimal control[J]. Transactions of the Chinese Society for Agricultural Machinery, 2013, 44(2): 165 - 170. (in Chinese)

6 Shoval S, Zyburt J P, Grimaudo D W. Robot driver for guidance of automatic durability road (ADR) test vehicles[C]// 1998 IEEE International Conference on Robotics and Automation, 1998, 2: 1767 - 1772.

7 陈刚, 张为公, 龚宗洋, 等. 汽车驾驶机器人多机械手协调控制研究[J]. 仪器仪表学报, 2009, 30(9): 1836 - 1840.
Chen Gang, Zhang Weigong, Gong Zongyang, et al. Coordinated control of multiple manipulators for vehicle robot driver[J]. Chinese Journal of Scientific Instrument, 2009, 30(9): 1836 - 1840. (in Chinese)

8 张为公, 陈晓冰. 汽车驾驶机器人关键技术[J]. 江苏大学学报: 自然科学版, 2005, 26(1): 20 - 23.
Zhang Weigong, Chen Xiaobing. Key technologies of vehicle robot driver[J]. Journal of Jiangsu University: Natural Science Edition, 2005, 26(1): 20 - 23. (in Chinese)

9 Matsumura T, Ichikawa S, Katsu F, et al. The development of a controller confirmation system for automatic transmissions and its applications[C]// Proceedings of the 2004 IEEE International Conference on Control Applications, 2004, 2: 1415 - 1419.

10 陈刚, 张为公, 常思勤. 汽车驾驶机器人模糊神经网络换挡控制方法[J]. 农业机械学报, 2011, 42(6): 6 - 11.
Chen Gang, Zhang Weigong, Chang Siqin. Shift control method of vehicle robot driver based on fuzzy neural network[J]. Transactions of the Chinese Society for Agricultural Machinery, 2011, 42(6): 6 - 11. (in Chinese)

11 金景苏, 李永军, 徐海平. 同步器在江苏 750 型拖拉机变速器中的应用[J]. 无线互联科技, 2015(7): 138 - 139.
Jin Jingsu, Li Yongjun, Xu Haiping. The application of synchronizer in Jiangsu 750 tractor transmission[J]. Wireless Internet Technolog, 2015(7): 138 - 139. (in Chinese)

12 周纪良. 拖拉机变速箱的结构型式和结构谱[J]. 农业机械学报, 1979, 10(2): 47 - 63.
Zhou Jiliang. Structure and spectrum of tractor transmission[J]. Transactions of the Chinese Society for Agricultural Machinery, 1979, 10(2): 47 - 63. (in Chinese)

13 He B, Han L, Wang Y, et al. Kinematics analysis and numerical simulation of a manipulator based on virtual prototyping[J]. The International Journal of Advanced Manufacturing Technology, 2014, 71(5 - 8): 943 - 963.

14 Udriste C, Tevy I. Multi-time Euler-Lagrange dynamics[C]// Proceedings of the 7th WSEAS International Conference on Systems Theory and Scientific Computation (ISTASC07), 2007: 66 - 71.

15 Liu Y C, Chopra N. Controlled synchronization of heterogeneous robotic manipulators in the task space[J]. IEEE Transactions on Robotics, 2012, 28(1): 268 - 275.

16 Heidarbeigi K, Ahmadi H, Omid M, et al. Evolving an artificial neural network classifier for condition monitoring of massy ferguson tractor gearbox[J]. International Journal of Applied Engineering Research, 2010, 5(12): 2097 - 2107.

17 Zhang J, Chen L, Xi G. System dynamic modelling and adaptive optimal control for automatic clutch engagement of vehicles[J]. Proc. IMech E Part D: Journal of Automobile Engineering, 2002, 216(12): 983 - 991.

18 陈玉祥. 基于虚拟样机技术的机械式变速器换挡性能仿真分析[D]. 广州: 华南理工大学, 2012.
Chen Yuxiang. Simulation analysis on the shifting performance of mechanical transmission based on virtual prototype technology[D]. Guangzhou: South China University of Technology, 2012. (in Chinese)

19 许祥, 侯丽雅, 黄新燕, 等. 基于外骨骼的可穿戴式上肢康复机器人设计与研究[J]. 机器人, 2014, 36(2): 147 - 155.
Xu Xiang, Hou Liya, Huang Xinyan, et al. Design and research of a wearable robot for upper limbs rehabilitation based on exoskeleton[J]. Robot, 2014, 36(2): 147 - 155. (in Chinese)

20 秦东晨, 王丽霞, 刘竹丽, 等. SQP 法在大型结构优化设计中应用的研究[J]. 河南科学, 2006, 24(3): 431 - 433.
Qin Dongchen, Wang Lixia, Liu Zhuli, et al. A study on SQP method application for large-scale structural optimization design[J]. Henan Science, 2006, 24(3): 431 - 433. (in Chinese)